Meteoritics & Planetary Science 37, 1591–1598 (2002)
Available online at http://www.uark.edu/meteor

Thermoluminescence of forsterite and fused quartz as a candidate for the extended red emission

C. KOIKE[1]*, H. CHIHARA[1,4], K. KOIKE[2], M. NAKAGAWA[2], M. OKADA[3], A. TSUCHIYAMA[4], M. AOKI[2], T. AWATA[5] AND K. ATOBE[5]

[1]Kyoto Pharmaceutical University, Kyoto 607-8412, Japan
[2]Faculty of Education, Kagawa University, Takamatsu 760-8522, Japan
[3]Research Reactor Institute, Kyoto University, Kumatori 590-0499, Japan
[4]Department of Earth and Space Science, Osaka University, Toyonaka 560-0043, Japan
[5]Faculty of Education, Naruto University of Education, Naruto, Tokushima 772-8502, Japan
*Correspondence author's e-mail address: koike@mb.kyoto-phu.ac.jp

(Received 2002 February 9; accepted in revised form 2002 August 9)
(Presented at "Laboratory Simulations of Circumstellar Dust Analogs: Expectations for Comet Nucleus Encounters", a special session of the 64th annual Meteoritical Society meeting, Vatican City, 2001 September 13)

Abstract–We investigated thermoluminescence of silicates that are of interest in the interstellar and circumstellar medium after irradiation by γ-rays and fast neutrons. The silicates are forsterite, orthoenstatite, olivine, quartz, and crystalline silicon. The irradiated enstatite shows weak and broad peaks at 545 and 760 nm. In contrast, irradiated bulk and powder samples of forsterite show strong and broad peaks at 640–660 nm. Although thermoluminescence of bulk forsterite is very similar to the extended red emission (ERE) of the Red Rectangle nebula, irradiated powdered forsterite did not reveal any sharp emission features over the broad band. Further, we investigated the possibility of thermoluminescence of crystalline silicon and found that luminescence scarcely appears. It is emphasized that the prominent carrier of ERE is forsterite and fused quartz.

INTRODUCTION

Extended red emission (ERE) is a broad emission band with a peak wavelength between 600 and 850 nm and with a width between 60 and 120 nm. It is seen in many dusty astrophysical objects such as reflection nebulae, planetary nebulae, HII regions, halos of galaxies, and even in the diffuse interstellar medium. The observation of ERE in the diffuse interstellar medium shows that ERE is a general phenomenon. Though the carrier for ERE is not yet clear, the proposed carriers are hydrogenated amorphous carbon (HAC), quenched carbonaceous composite (QCC), C_{60}, carbon nanoparticles, polycyclic aromatic hydrocarbons (PAHs), and silicon nanoparticles, and most of them appear to be unable to explain the observed ERE spectra (see Ledoux *et al.*, 2001; Witt *et al.*, 1998, for a summary).

Recently, we have suggested that thermoluminescence spectra of forsterite after γ-ray irradiation are very similar to the ERE of the Red Rectangle nebula (Koike *et al.*, 2002). In this paper, we will investigate this possibility in more detail. We especially examined powdered forsterite, enstatite, fused quartz and crystalline silicon. We propose that the thermoluminescence is related to changes in the properties of interstellar and circumstellar matter and of the accumulated energy by varied irradiation in interstellar and circumstellar space.

Interstellar and circumstellar matter is irradiated by high-energy electromagnetic and cosmic-ray particles, such as γ-rays, neutrons, protons, heavy ions, *etc.* These forms of irradiation will cause some changes to these materials, such as their optical properties. It is especially known that extremely large fluxes of neutrons and γ-rays have been emitted during supernova explosions. Furthermore, interstellar and circumstellar space is typically at extremely low temperature and is being constantly irradiated by electromagnetic radiation and by cosmic-ray particles for long time periods. The effects of this radiation will accumulate in the low-temperature environment.

In the circumstellar region of both young and evolved stars, as well as in the solar system, forsterite and enstatite have been found (Waters *et al.*, 1998a,b; Malfait *et al.*, 1998; Wooden *et al.*, 1999) by the infrared space observatory (ISO) (Kessler *et al.*, 1996). Carbonates such as dolomite ($CaMg(CO_3)_2$), breunnerite ($Mg(Fe,Mn)(CO_3)_2$), calcite ($CaCO_3$), and Mg,Ca-bearing siderite ($FeCO_3$) have been found in CI chondrite (Endress *et al.*, 1996). Among these carbonates, Ca-bearing minerals such as dolomite and calcite have also been detected in dust shells around evolved stars by the ISO (Kemper *et al.*, 2002). It should be especially noted that the broad emission

Prelude preprint MS#4765

feature responsible for ERE appears at about the 600–900 nm region in many reflection nebulae. Among reflection nebulae, the Red Rectangle nebula shows the strongest intensity by 1 order, and sharp emission features at near 580, 638, and 662 nm over a broad band (Witt and Boroson, 1990). In the Red Rectangle nebula, both PAH and crystalline silicates (forsterite and enstatite) features were observed by the ISO (Waters *et al.*, 1998b).

We have suggested, on the basis of the measurement of thermoluminescence for irradiated silicates and carbonates, our thermoluminescence spectra of forsterite at 645–655 nm and at 590 nm are very similar to the ERE of the Red Rectangle nebula (Koike *et al.*, 2002). The spectra were, however, obtained only from bulk samples of forsterite, and not compared with other silicates such as quartz in general. In this paper, we will investigate the properties of silicates in the context of astrophysics, where thermoluminescence spectra after γ-ray and neutron irradiation are compared in detail. In order to reveal any size effects on thermoluminescence, detailed thermoluminescence spectra of powdered forsterite are also measured. Further, the problem of silicon nanoparticles is also discussed.

EXPERIMENT

Irradiation by Gamma-Rays and Neutrons

The γ-ray irradiated bulk samples are forsterite (Mg_2SiO_4), orthoenstatite ($MgSiO_3$), natural olivine (Fo_{90}), synthesized fused quarts (SiO_2) and crystalline silicon (Si). Two bulk samples of forsterite were named bulk1 and bulk2, (7 × 8 mm, 2 mm thick) and 245 mg, and (7 × 10 mm, 1 mm thick) and 138 mg, respectively. Natural olivine are two samples from San Carlos and Egypt. Fused quartz and crystalline silicon samples are all commercial products. In order to study the size effects on thermoluminescence, powder samples are also prepared which are powdered forsterite and powder-pressed forsterite. These samples are irradiated with γ-rays to a dose of ~10.4×10^4 Ga (J/Kg) in liquid nitrogen using the ^{60}Co γ-ray irradiation facility of Kyoto University Reactor (KUR). The γ-rays of ^{60}Co have two peaks at 1.1 and 1.3 MeV. Our samples of forsterite and enstatite were synthesized single crystals using the CZ (Czochralski) (Takei and Kobayashi, 1974) and Flux method (Tachibana, 2000), respectively.

We also investigated the effect of irradiation on a bulk sample of forsterite (named bulk3) of fast neutrons to a dose of 8×10^{16} n_f/cm^2 at 10 and 70 K using the low-temperature irradiation facility of KUR (Okada *et al.*, 2001). After fast neutron irradiation for 75 h, samples were stored in liquid nitrogen for several months to allow for a decay of radioactivity.

We have measured the thermoluminescence spectra of these samples using a spectrophotometer (Princeton Instruments, Inc., at KUR). The sample is put on a thermally isolated plate, which had previously been cooled to liquid nitrogen temperature. The luminescence emission during warming is measured with a charge-coupled device (CCD) measuring system using an optically transparent fiber. The duration time for samples warming from liquid nitrogen to room temperature is ~15 min. It should be noted that this time length is sufficient to observe the thermoluminescence, where photons are emitted at the thermal equilibrium state. The measured data points are set same in general, but only in the case of strong or weak intensity those points are set to change.

In the interstellar and circumstellar environment, irradiations are repeated over and over again. In order to simulate similar conditions, after measurements of thermoluminescence, the γ-ray irradiation on these samples were repeated, or further repeated after several months or half a year later, of which samples were forsterite (bulk1, bulk2) and orthoenstatite.

The Intensity of Thermoluminescence

All data were measured under almost identical conditions: identical device, setting and warming time of 15 min. It is very difficult to measure the absolute intensity of luminescence, because the absolute number of photon emitted as luminescence is hard to quantify. Thus, the relative intensity of luminescence to the background fluctuations may be one indicator for comparing the intensity of each sample. In this paper, all data are normalized with the background fluctuations of each samples, and with measured time of 100 s.

RESULTS

Luminescence of Forsterite and Enstatite

The luminescence spectra are shown for γ-ray irradiated and neutron-irradiated forsterite in Fig. 1. The luminescence intensity of γ-ray irradiated samples are strong compared to that of neutron-irradiated samples. For the spectra after γ-ray irradiation, a rather intense broad peak at 640–655 nm and a weak broad peak at 420–440 nm are detected. This feature is common to all bulk samples and powder ones. In addition, in the case of bulk samples, other weak peaks at 590, 595, and 705 nm also appeared (Koike *et al.*, 2002).

We have confirmed the reappearance of spectra in two bulk samples (bulk1 and bulk2) and in re-irradiated samples. The reappearance of spectra of maximum intensity for two bulk samples (bulk1 and bulk2) are shown in Fig. 1. The spectra after γ-ray irradiation repeated a second and third times on bulk1 are also shown as green and red lines, respectively. As for the bulk2 sample, its spectra after irradiation was weak, but the spectra after re-irradiation became stronger and showed a fine structure (Fig. 1 in Koike *et al.*, 2002). After further re-irradiation, the reappearance of the fine structure was also confirmed, although the spectra was saturated at around maximum intensities due to strong intensities. In Fig. 1, the intensity of the bulk1 sample after the first and third irradiation

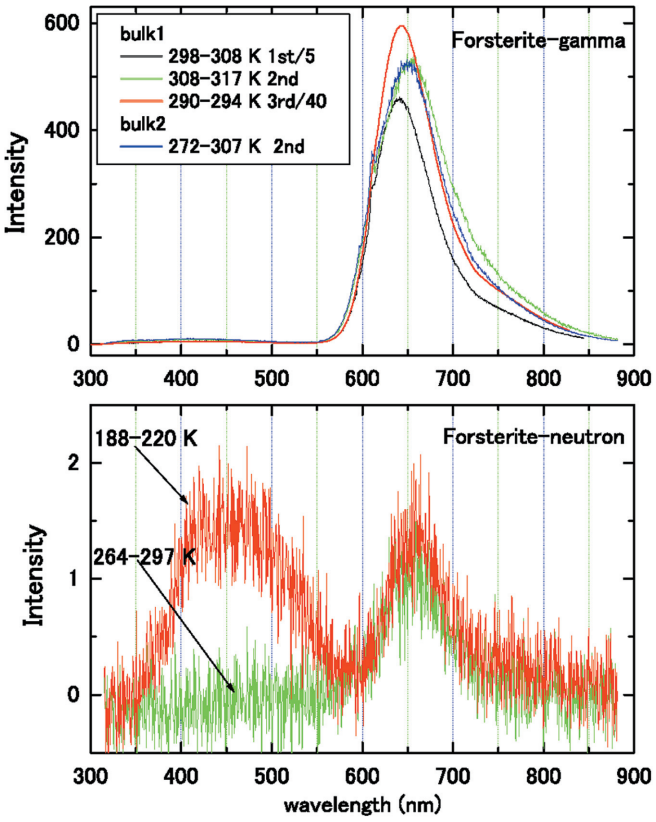

FIG. 1. Thermoluminescence spectra of single crystals of forsterite after γ-ray (upper panel) and neutron irradiation (lower panel). The γ-ray irradiated spectra show in the case of maximum intensity for two bulk samples (bulk1 and bulk2) and re-irradiated bulk1 sample (green line and red line), of which black line and red line are scaled down by a factor of 5 and 40, respectively, than the original intensity, because the intensity was very strong. In the lower panel, only typical spectra are shown for neutron-irradiated forsterite (bulk3).

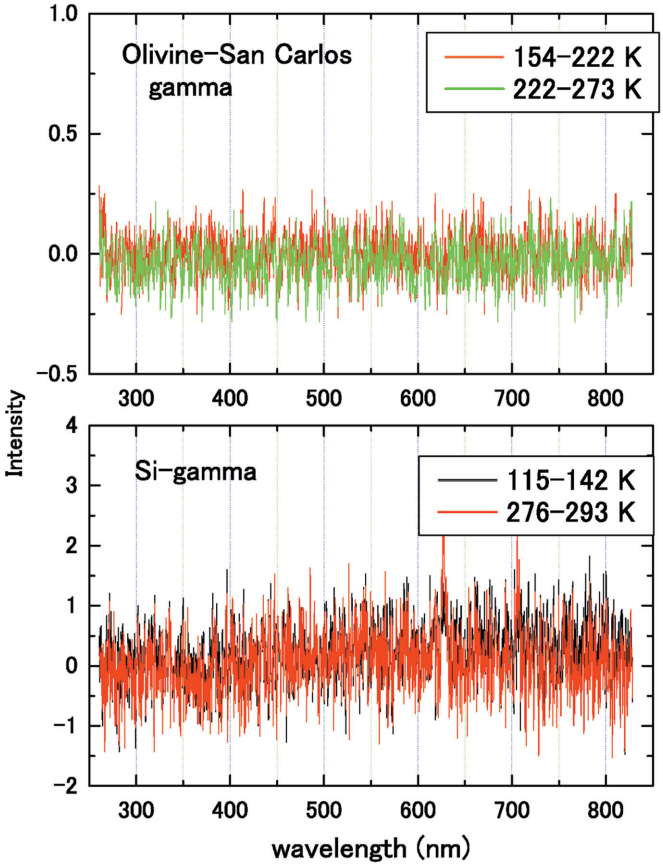

FIG. 2. Thermoluminescence spectra of olivine from San Carlos (upper panel) and crystalline silicon (lower panel). The spectra of these two samples are independent of warming temperature.

is scaled down by a factor of 5 and 40 relative to the original spectra, respectively. The intensity of the bulk1 and bulk2 samples after they were irradiated for a third time was the strongest, and sharp features at 590, 595, and 705 nm were hidden because of large intensity of broad band when the intensity of spectra became maximum. The width of 650 nm band became narrow or broad when the intensity of the band became strong or weak, respectively. The intensity of the broad band at 640–655 nm seems to become stronger as repeated γ-ray irradiation, except in the case of re-irradiated (second) bulk1.

The intensity of broad band at 420–440 nm also became stronger after repeated γ-ray irradiation, and it became prominent at room temperature, where the intensity is nearly the same or stronger than another broad band at 640–660 nm. The broad band at 640–655 nm appears also in the spectra of neutron irradiation. The most characteristic point of neutron irradiation is the intensity of the broad band at 430–470 nm, which has a comparable strength with the intensity of the broad band at 645–655 nm in the case of low temperature at about 188–220 K.

In contrast, the luminescence is scarcely visible in natural olivine (Fo_{90} from San Carlos and Egypt) as shown in Fig. 2. These samples are one bulk (several millimeters in size) and several small particles (millimeter size) for San Carlos and for Egypt, respectively.

We have also examined the thermoluminescence spectra of powdered forsterite (several tens of microns in size) in detail (Fig. 3). The result is almost the same as the bulk. However, the weak peaks at 590, 595, and 705 nm became weaker and did not appear. The fine peaks did not appear even at low or high temperature, at which the intensity of broad band was weak. The temperature at maximum intensity for powdered forsterite was 156–166 K, and low compared with that of bulk samples (272–317 K) (Fig. 1). We have examined the spectra of powder-pressed forsterite, and the luminescence is the same as powdered forsterite, but the temperature at maximum intensity was 172–187 K, slightly higher than for the powder samples. The temperature at maximum intensity seems to depend on sample size (*i.e.*, the temperature for small size samples seems to become low compared with that for bulk samples).

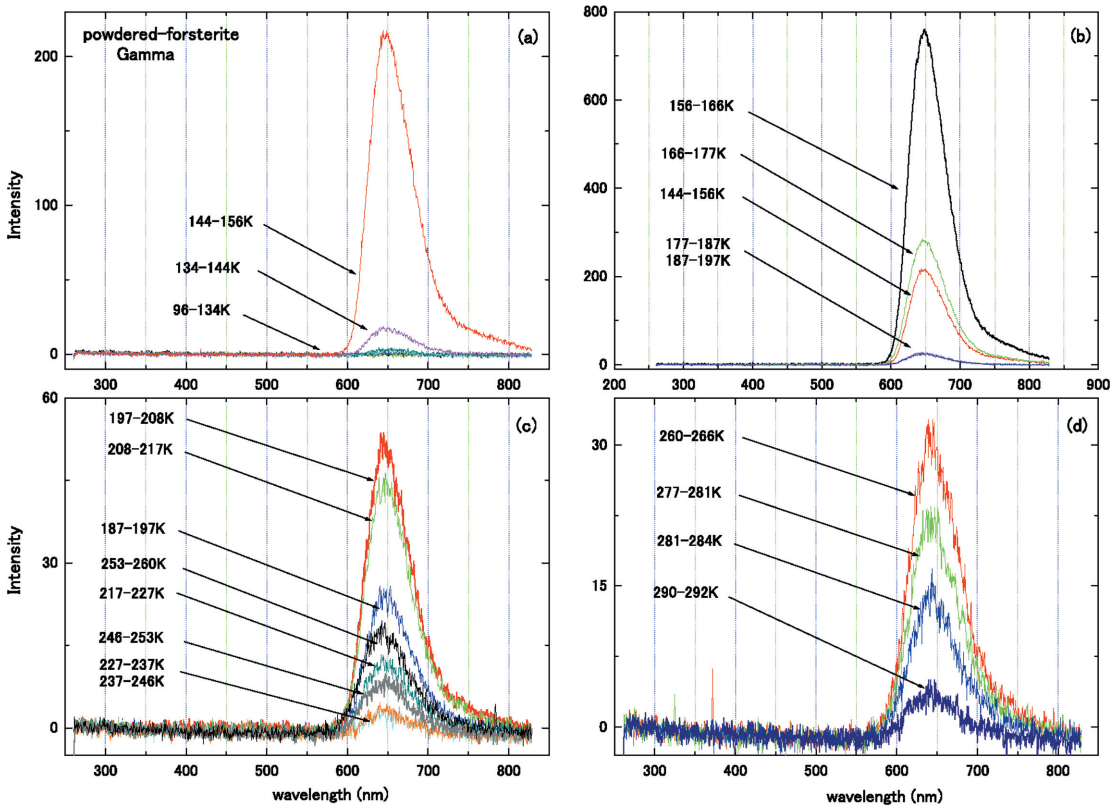

FIG. 3. Detailed thermoluminescence spectra of powdered forsterite. The warming temperature increases from panels (a) to (d). The intensity becomes strong at 144–177 K and strongest at 156–166 K, but at higher temperature, the intensity suddenly grew weak.

We have examined the luminescence spectra for re-irradiated enstatite in detail, which are shown in Fig. 4. The orthoenstatite samples are several fragments: 1–2 mm in size and 114 mg. Two broad peaks appear at 545 and 760 nm, and these peaks are weak compared with that of forsterite. These luminescences are somewhat different from our previous spectra (Koike *et al.*, 2002), in which the broad peak at 550 nm became weaker than the broad peak at 760 nm. These may be due to remaining defects. Because after γ-ray irradiation, the luminescence of enstatite samples were measured during warming from liquid nitrogen temperature to ~380 K, and γ-ray was further re-irradiated several months later. The luminescence of enstatite after γ-ray irradiation for the first time was almost zero, whereas the intensity of the previous spectra and the present spectra increased after re-irradiation for the second time, and for the third time, respectively, due to remaining defects.

We have also measured the thermoluminescence spectra of γ-irradiated bulk sample of fused quartz (10 mm diameter, 1 mm thick), which are shown in Fig. 5. The peak is at ~660 nm and resembles that of forsterite. In contrast, in the case of γ-irradiated bulk samples of crystalline silicon (~10 mm diameter, 0.4 mm thick), thermoluminescence scarcely appears (Fig. 2).

DISCUSSION

Extended Red Emission and Silicates

In a previous paper (Koike *et al.*, 2002), we have pointed out that the luminescence of forsterite is very similar to ERE of the Red Rectangle nebula (peak at 652–684 nm, half width 70–90 nm). Generally speaking, ERE from interstellar dust consists of a broad, featureless emission band peaking at 610–820 nm with a 60–100 nm width. Among many objects, the Red Rectangle nebula shows stronger emission by 1 order and exhibits the sharp emission features over a broad band. Furthermore, crystalline silicates such as forsterite and PAH dust have been founded in the Red Rectangle nebula by the ISO (Waters *et al.*, 1998b). It should also be noted that forsterite and enstatite have been found by the ISO in many oxygen-rich young and evolved stars. However, in general, ERE is observed in carbon-rich stars. It is important to note that the Red Rectangle nebula is a very interesting object with both carbon- and oxygen-rich characteristics, where both forsterite and PAH can be found. It is remarkable fact that the observed spectra of ERE of the Red Rectangle nebula (Witt and Boroson, 1990) shows the sharp emission features over a broad band at, or near 580, 638, and 662 nm.

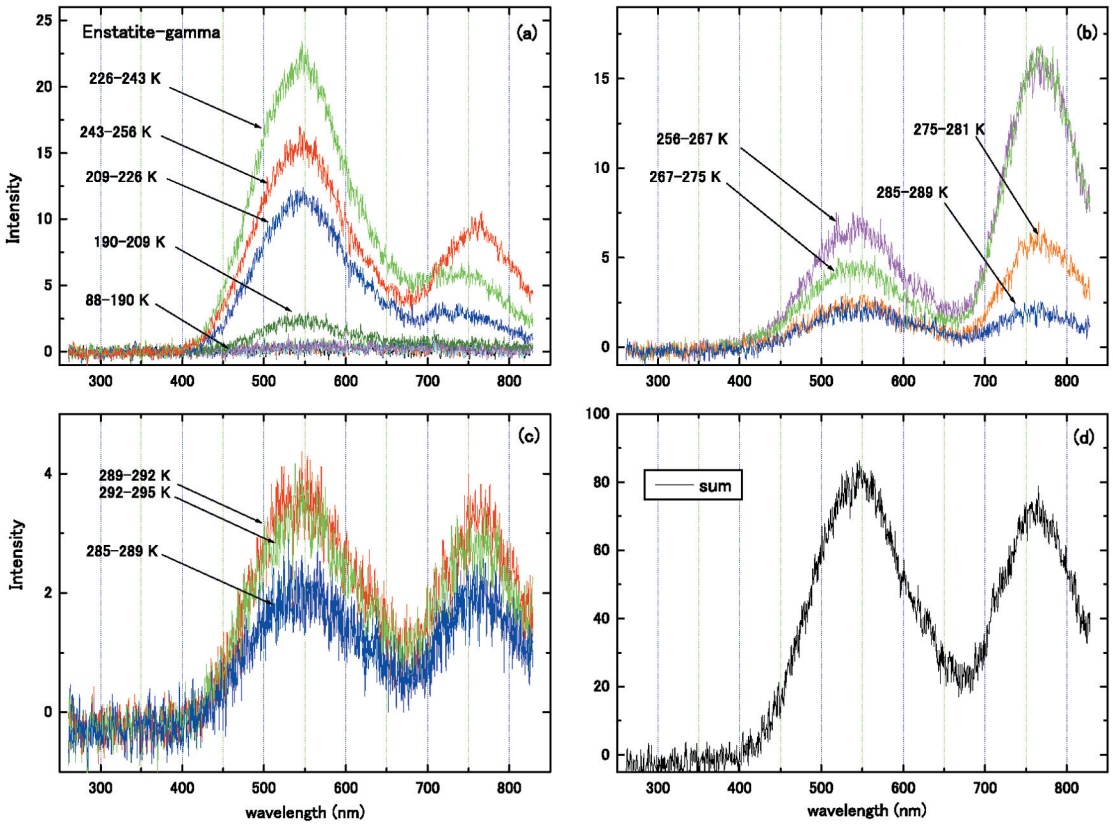

FIG. 4. Detailed thermoluminescence spectra of single crystals of orthoenstatite. (a) The peak intensity at 550 nm becomes strongest at 226–243 K, and weaker as the temperature goes higher. The peak intensity at 760 nm becomes strongest at 256–267 and 267–275 K. After those temperatures, the peak intensity becomes weak (b), and the peak intensity of both peaks at 550 and 760 nm are identical (c). Total intensity of both peaks are shown in (d).

The typical thermoluminescence spectra of forsterite in bulk and powder are compared with ERE of the Red Rectangle nebula in Fig. 6. The width of spectra seems to depend on the intensity and/or warming temperature of the irradiated forsterite, which means the width becomes narrow at around the maximum intensity. So, the rather broad spectra with fine structure appeared at low or high temperature in the case of the bulk samples. In Fig. 6, the spectra of bulk1 (at 336–366 K, after re-irradiated), bulk2 (at 116–122 K, after irradiated for a third time), and powder (at 187–217 K) are shown.

Among our irradiated samples, forsterite of both bulk and powder show very intense luminescence (peak at 640–660 nm) by several orders than other samples, and half-width of about 60–100 nm as shown in Figs. 1 and 3, with fine structures at 590, 595, and 705 nm in the case of the bulk samples. The fine structures did not appear in the case of powdered forsterite and seems to appear in the case of adequate size. If so, the adequate size of forsterite larger than powder size may also exist in the Red Rectangle nebula as well as submicron size of forsterite, because observed ERE shows the fine structure (Fig. 6). It should be reemphasized that our thermoluminescence spectra of forsterite at about 645–655 nm and at 590 nm are very similar to the ERE of the Red Rectangle nebula. As for carriers of ERE, a possible size effect of crystalline silicon nanoparticles has been discussed (Ledoux *et al.*, 2001). It has been shown that the photoluminescence spectra of these nanoparticles can explain the gross structure of the ERE spectra, such as the peak position and the full width at half-maximum of ERE spectra, *etc*. However, evidence of existence of crystalline silicon has not yet been observed (Li and Draine, 2001, 2002).

In Figs. 2 and 5, we show the thermoluminescence spectra of silicon and fused quartz. It should be remembered that the spectra of fused quartz resembles that of forsterite; however, the fine structure such as the weak peak at 590 nm does not appear in the spectra of fused quartz. The gross structure such as the position of main peak and the half-width is almost similar to that of forsterite except for a subtle difference. In contrast, thermoluminescence appears scarcely in the case of crystalline silicon.

As a result, considering both our works and the discussion of Li and Draine (2001, 2002), we would like to propose that the prominent carrier of ERE is crystalline forsterite and SiO_2.

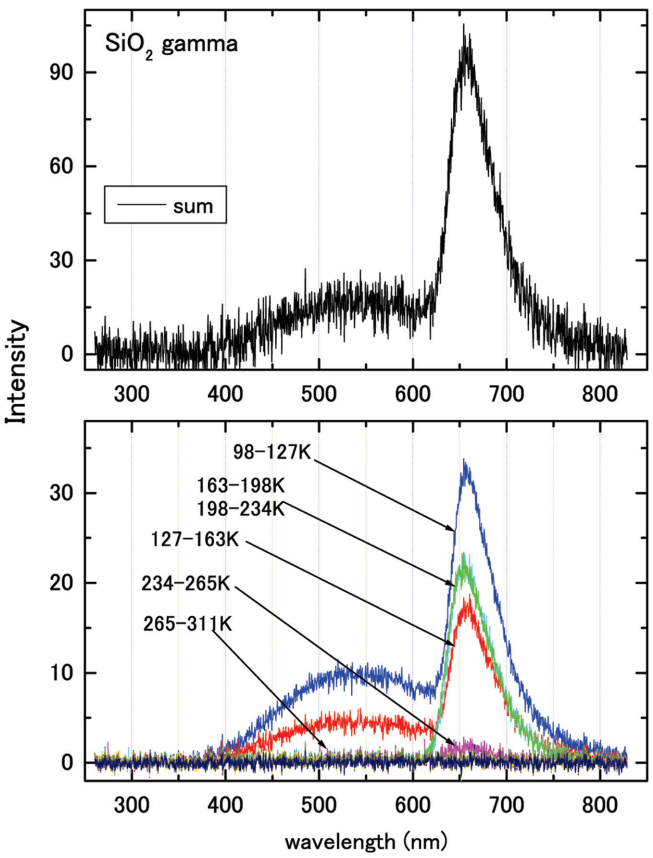

FIG. 5. Thermoluminescence spectra of fuse quartz. The peak is at ~660 nm and resembles that of forsterite. Lower and upper panels show the spectra depending upon temperature and total intensity, respectively.

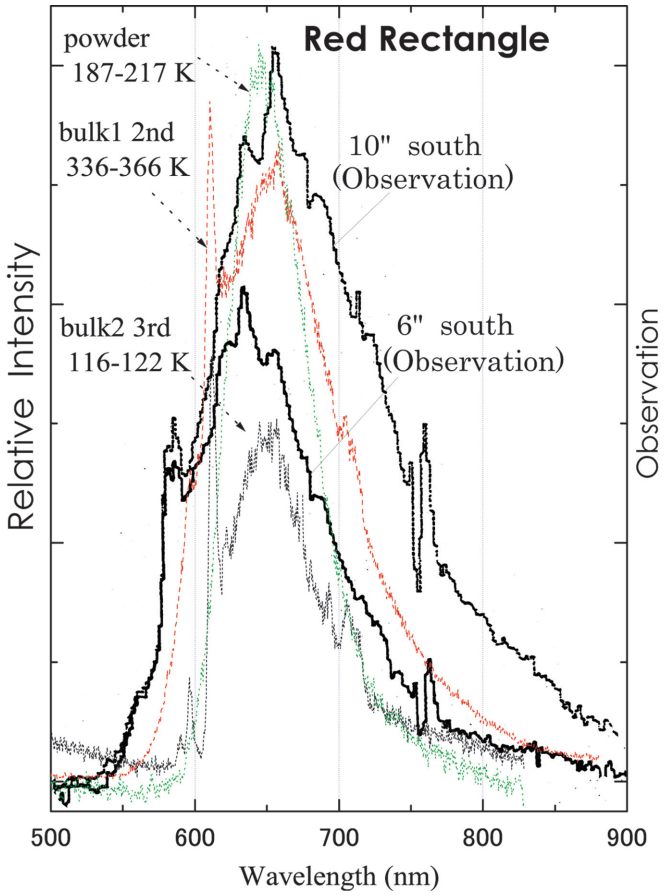

FIG. 6. Comparison with the observed ERE spectra of the Red Rectangle nebula (from Witt and Boroson, 1990) and forsterite spectra (bulk1, bulk2, and powder). Observed spectra are full lines indicated by line 6", 10" south. Forsterite spectra are dotted lines indicated by dotted arrow.

The Effect of Minor Elements

Among the samples, the intensity of thermoluminescence of forsterite was the strongest; in contrast, those of natural olivine were near zero and had no feature. The chemical composition of natural olivine from San Carlos and Egypt is Fo_{90} and FeO content is ~10%. In connection with the difference of chemical composition from olivine, the cathodoluminescence (CL) of forsterite with less than ~2% FeO from carbonaceous chondrite (Steele, 1986, 1989) is worth noticing. Under electron bombardment, some minerals emit light, which is called cathodoluminescence. Following the works by Steele (1986, 1989), the spectra of forsterite with <2% FeO show blue CL (at ~450 nm) and red CL (at ~800 nm), but those of Fe-rich olivine show extremely weak features. The intensity of the blue CL peak is very weak at FeO concentrations greater than 1%. The red CL peak and intensity correlate inversely with the concentration of Mn and Fe. The red intensity nears 0 for ~2% FeO in contrast to 0.75% for blue. The thermoluminescence of natural olivine after γ-ray irradiation shows almost no feature, which may be due to high FeO concentration. It is very interesting to note whether the intensity and peak position of thermoluminescence changes and shifts in the case of forsterite with FeO concentrations smaller than 2% similar to the red CL of forsterite from chondrites. The broad peak position between 600 and 850 nm may be explained by considering both CL and thermoluminescence from minor trace elements in forsterite.

Possible Heat Source of Thermoluminescence

It should be noted that interstellar and circumstellar space is typically at extremely low temperature and is constantly being irradiated by electromagnetic radiation and by cosmic-ray particles for long time periods. Furthermore, it is well known that extremely large fluxes of neutrons and γ-rays have been emitted during supernova explosions. The effect of this radiation will accumulate in the low-temperature environment. It will only be observed if the condition to release the accumulated energy is realized in circumstellar space. This may be occur when irradiated dusts become warm in interstellar or circumstellar environment.

As for the stability of accumulated energy, the study of red thermoluminescence in archaeology is very interesting. It is estimated that accumulated energy in SiO_2 by natural radioactivity, such as cosmic rays, is almost stable for more than 10^6 year in the Earth's surface environment (Hashimoto *et al.*, 1993, 1999). In extremely low-temperature environments, the effects of irradiation may be "frozen" and almost stable for extremely long times, and various irradiation effects, such as those often observed with supernova explosions or irradiating cosmic rays, may accumulate. The accumulated energy in irradiated matter is released as thermoluminescence when the matter is warmed. The irradiation of matter generally cause lattice defects in crystals, and a certain kind of this effect is observed in thermoluminescence. It is known in many experiences that the irradiation effect in solids can be erased by warming it to several hundred degrees Celsius. In other word, the effects of irradiation remains in a certain kind of state below this temperature and it may be observed as further remaining effects different from the thermoluminescence.

The heating process such as shock heating or ultraviolet irradiation may raise the temperature of the irradiated matter. The shock heating may arise from grain–grain, gas–gas, grain–gas, or electron–dust collisions in a turbulent disk environment. In optically thin environments, irradiated ultraviolet photons on grains may raise the temperature. Our preliminary experiments show that the ultraviolet irradiation led the strong luminescence. After ultraviolet photons were radiated on the γ-ray irradiated forsterite sample at room temperature, the forsterite emitted red light, which can be easily seen with the naked eye, and a strong luminescence spectra was seen as in Fig. 1. The luminescence was shown only within several months after heating up to 380 K for γ-ray irradiated forsterite sample. These works are now in progress (C. Koike *et al.*, unpubl. data).

CONCLUSION

In this paper, we have emphasized that forsterite and fused quartz are the prominent carriers of ERE. Detailed thermoluminescence spectra are shown for enstatite and powdered forsterite, and compared with that of fused quartz. These investigations are an extension of our previous work (Koike *et al.*, 2002), in which we have pointed out that the spectra of forsterite at about 645–655 nm and at 590 nm is very similar to the ERE of the Red Rectangle nebula. It should be noted that size effect of crystalline silicon nanoparticles can explain the gross structure of the ERE spectra (Ledoux *et al.*, 2001). However, this model can not explain the sharp emission features at 590 nm of ERE. The interesting fact of this size effect is that the peak of gross structure of luminescence shifts depending on the size of nanoparticles.

We have examined the possible thermoluminescence in both crystalline silicon and fused quartz as shown in Figs. 2 and 5. The luminescence of fused quartz resembles that of forsterite, except for the sharp emission features over a broad band, whereas luminescence scarcely appears in crystalline silicon. The characteristic difference between forsterite and silicon is that the irradiated energy is accumulated or not, and that this accumulation will be observed as thermoluminescence under a certain kind of condition. From this viewpoint, it is interesting to examine the possible existence of similar size effect in fused quartz and forsterite nanoparticles, which existence was examined in Si by Ledoux *et al.* (2001). The difference between bulk and powdered forsterite appears in whether it shows fine structure or not. Taking into account of the feature of ERE of the Red Rectangle nebula, it seems that the rather large size of forsterite may exist together with submicron size one in the Red Rectangle nebula.

Investigating the reason for differences in thermoluminescence spectra among bulk, powder and nanoparticles samples is a further problem.

Acknowledgments–We would like to thank anonymous referees for useful comments concerning CL of forsterite and constructive discussion. This work was supported by the KUR projects (12062, 13P1-6). Part of this work was supported by Grant-in-Aid of Japanese Ministry of Education, Science, and Culture (12440054).

Editorial handling: D. W. G. Sears

REFERENCES

ENDRESS M., ZINNER E. AND BISCHOFF A. (1996) Early aqueous activity on primitive meteorite parent bodies. *Nature* **379**, 701–703.

HASHIMOTO T. *ET AL.* (1993) Activation energies from blue- and red-TL of quarts grains and mean lives of trapped electrons related to natural red-TL. *Nucl. Tracks Radiat. Meas.* **21**, 217–223.

HASHIMOTO T., FUJITA H. AND YASUDA K. (1999) Mean-life evaluation of naturally trapped electron associated with red- and blue-thermoluminescent dune sand. *RadioIsotope* **48**, 673–682.

KEMPER F. *ET AL.* (2002) Detection of carbonates in dust shells around evolved stars. *Nature* **415**, 295–297.

KESSLER M. F. *ET AL.* (1996) The Infrared Space Observatory (ISO) mission. *Astron. Astrophys.* **315**, L27–L31.

KOIKE K., NAKAGAWA M., KOIKE C., OKADA M. AND CHIHARA H. (2002) Thermoluminescence of simulates interstellar matter after gamma-ray irradiation: Forsterite, enstatite and carbonates. *Astron. Astrophys.* **390**, 1133–1139.

LEDOUX G. *ET AL.* (2001) Crystalline silicon nanoparticles as carriers for the extended red emission. *Astron. Astrophys.* **377**, 707–720.

LI A. AND DRAINE B. T. (2001) On ultrasmall silicate grains in the diffuse interstellar medium. *Astrophys. J.* **550**, L213–L217.

LI A. AND DRAINE B. T. (2002) Are silicon nanoparticles an interstellar dust component? *Astrophys. J.* **564**, 803–812.

MALFAIT K. *ET AL.* (1998) The spectrum of the young star HD 100546 observed with the infrared space observatory. *Astron. Astrophys.* **332**, L25–L28.

OKADA M. *ET AL.* (2001) Improvement of low-temperature irradiation facility at Kyoto University Reactor (KUR). *Nucl. Instrum. Methods Phys. Res.* **A463**, 213–219.

STEELE I. M. (1986) Cathodoluminescence and minor elements in forsterites from extraterrestrial samples. *Am. Mineral.* **71**, 966–970.

STEELE I. M. (1989) Compositions of isolates forsterites in Ornans (C3O). *Geochim. Cosmochim. Acta* **53**, 2069–2079.

TACHIBANA S. (2000) Incongruent evaporation kinetics of enstatite ($MgSiO_3$) and Mg/Si fractionation in the primitive solar nebula. Ph.D. thesis, Osaka University, Osaka, Japan. 150 pp.

TAKEI H. AND KOBAYASHI T. (1974) Growth and properties of Mg_2SiO_4 single crystals. *J. Crystal Growth* **23**, 121–124.

WATERS L. B. F. M. *ET AL.* (1998a) Crystalline silicates in planetary nebulae with [WC] central stars. *Astron. Astrophys.* **331**, L61–L64.

WATERS L. B. F. M. *ET AL.* (1998b) An oxygen-rich dust disk surrounding an evolved star in the Red Rectangle. *Nature* **391**, 868–871.

WITT A.N. AND BOROSON T. A. (1990) Spectroscopy of extended red emission in reflection nebulae. *Astrophys. J.* **355**, 182–189.

WITT A. N., GORDON K. D. AND FURTON D. G. (1998) Silicon nanoparticles: Source of extended red emission? *Astrophys. J.* **501**, L111–L115.

WOODEN D. H. *ET AL.* (1999) Silicate mineralogy of the dust in the inner coma of comet C/1995 (Hale–Bopp) pre-and post-perihelion. *Astrophys. J.* **517**, 1034–1058.